



Improved synthetic method of Benzo[a]pheno-selenazinium phototherapeutic agents

Xiuxiu Yue^a, Jing Xu^a, Xiaozhong Liu^b, Xiangzhi Song^{a,c,*}, James W. Foley^d

^a College of Chemistry & Chemical Engineering, Central South University, Changsha, 410083, Hunan Province, China

^b Medoncare Pharmaceutical Company Ltd. Changsha, 410205, Hunan Province, China

^c Key Laboratory of Hunan Province for Water Environment and Agriculture Product Safety, Changsha, 410083, Hunan Province, China

^d Rowland Institute at Harvard, Harvard University, Cambridge 02142, Massachusetts, USA

ARTICLE INFO

Keywords:

Photodynamic therapeutic agents
Benzo[a]phenoselenazinium dye
CuO nanopowder
Singlet oxygen
Improved synthesis

ABSTRACT

Benzo[a]phenoselenazinium dyes are excellent photodynamic therapeutic agents that have a red absorption (660 nm), high singlet oxygen quantum yield (>0.8), and good water-solubility and liposolubility. Bis-(3-diethylaminophenyl) diselenide, the most important intermediate for the synthesis of benzo[a]phenoselenazinium dyes, is previously prepared in one pot through 3 steps, during which special care is needed for the preparation of Grignard reagent and toxic selenium vapor. In this work, we employed CuO nanopowder to directly couple haloaniline with selenium to obtain pure bis-(3-diethylaminophenyl) diselenide (one step) under a mild condition with a high reaction yield without the need of column chromatography. Four benzo[a]phenoselenazinium dyes, **5a-d**, were easily prepared using the improved synthesis method; and their phototoxicity in living cells were investigated. The improved method could be employed in large-scale synthesis of benzo[a]phenoselenazinium dyes, thereby may stimulate the photodynamic study of this type of photosensitizer.

1. Introduction

As a treatment that has low toxicity, low cost and minimal invasiveness, but high effectiveness and dual selectivity, photodynamic therapy (PDT) is a promising alternative therapy for ophthalmologic, dermatologic, and cancerous oral lesions, head and neck cancers, bladder carcinoma, and a variety of intraperitoneal carcinomatosis and sarcomatous transformation [1–11]. In PDT, photosensitizers (PSs) are the key components which can be excited by absorbing photons so that they can subsequently react with oxygen to generate reactive oxygen species (ROS) such as singlet oxygen, superoxide anion radicals, hydroxyl radicals, and so on. Singlet oxygen (¹O₂) is the main ROS that can kill cancer cells through multifactorial mechanisms, such as stimulation of the inflammatory and immune responses [12–21]; therefore, photosensitizers with high singlet oxygen quantum yield are desirable. We first developed a new photodynamic therapeutic agent, benzo[a]phenoselenazinium dye **EtNBSe**, an effective photosensitizer that treats cutaneous leishmaniasis, tuberculosis and *Mycobacterium bovis* by oxidative damage [22–25]. Following the development, more studies on the derivative of **EtNBSe** have also been conducted [26–28]. All these studies have shown that benzo[a]phenoselenazinium photosensitizers

are highly suitable for photodynamic therapy *in vivo* because they have a red absorption in the optical window (600–900 nm), a high single oxygen quantum yield, good water-solubility and liposolubility, and excellent photo-stability [29–32].

We have previously synthesized benzo[a]phenoselenazinium dyes in six steps [25], as illustrated in **Scheme 1**. First, iodoaniline is converted into the Grignard reagent (3-diethylamino) phenylmagnesium iodide that subsequently reacts with selenium powder, is oxidized with air, and is finally nitrosated to produce bis-(3-diethylamino-6-nitrosophenyl) diselenide. Bis-(3-diethylamino-6-nitrosophenyl) diselenide is then condensed with 1-naphthylamine derivatives to afford dye **EtNBSe**. Although it was a successful approach, the synthesis of the key intermediate bis-(3-diethylaminophenyl) diselenide requires harsh conditions during the following two steps: i) the preparation and handling of the Grignard reagent (3-diethylamino) phenylmagnesium iodide requires a very dry environment; and ii) during the air oxidation process, toxic selenium vapor is produced, and aqueous sodium hypochlorite is needed to trap and bleach the vapor. In order to prepare more **EtNBSe** analogue dyes at a larger scale for use in intensive medical studies, there is a high demand for the neat synthesis under mild reaction conditions.

In this work, we improved the preparative process of bis-(3-

* Corresponding author. College of Chemistry & Chemical Engineering, Central South University, Changsha, 410083, Hunan Province, China.
E-mail address: xzsong@csu.edu.cn (X. Song).

<https://doi.org/10.1016/j.dyepig.2021.109154>

Received 14 November 2020; Received in revised form 13 January 2021; Accepted 13 January 2021

Available online 18 January 2021

0143-7208/© 2021 Elsevier Ltd. All rights reserved.

diethylaminophenyl) diselenide with an aim to increase the level of the synthesis of EtNBSe derivatives to a larger scale (Scheme 2).

2. Experimental

2.1. Instruments and materials

^1H NMR and ^{13}C NMR spectra were on a Bruker 400 spectrometer; the chemical shifts were reported in ppm in relative to those of TMS (tetramethyl silicane), an internal standard. Mass spectra were acquired using a Bruker Daltonics micrOTOF-Q II mass spectrometer. Absorption and emission spectra were recorded on Hitachi F-7000 fluorometer and Shimadzu UV-2450 spectrophotometer, respectively. Unless otherwise stated, all reagents were used as received. Twice-distilled water was used in all experiments.

2.2. Synthesis of CuO nanopowder

Fifty milliliters of aqueous CuSO_4 solution (0.5 M) was mixed by stirring with 50.0 mL of aqueous NaOH solution (1.0 M) in a beaker; immediately after mixing, blue flocculent precipitate was formed. Next, add 130.0 mL of sodium carbonate aqueous solution (0.5 M) to the mixture, and continue to stir for 30 min. Collect the precipitate by filtration and then wash with distilled H_2O until SO_4^{2-} was no longer detected by BaCl_2 . The obtained solid was dried in an oven at 90°C for 3 h and was then ground into powder. Finally, the powder was calcined at 350°C for 4 h from which black CuO nanopowder was obtained.

2.3. Synthesis of bis-(3-diethylaminophenyl) diselenide (2)

Under argon atmosphere and while being stirred, powdered Se metal (9.53 g, 120.0 mmol), CuO nanoparticles (0.46 g, 6.0 mmol) and KOH (6.74 g, 120.0 mmol) were added to a solution of 3-iodo-N, N-diethyl-aniline (1) (16.5 g, 60.0 mmol) in dry DMSO (60.0 mL). The mixture was then heated to 110°C overnight. After cooling down to room temperature, 10.0 mL of water was added. After that, the reaction mixture was extracted three times with ethyl acetate (3 x 40.0 mL). The organic phase was washed twice with brine and thereafter dried over anhydrous Na_2SO_4 overnight. After ethyl acetate was removed under a reduced pressure, light red oil (20.35 g, 74%) was obtained.

2.4. Synthesis of bis-(3-diethylamino-6-nitrosophenyl) diselenide (3)

In an ice-water bath, a solution of NaNO_2 (6.20 g, 98.2 mmol) in 80.0 mL water was added dropwise to a solution of bis-(3-diethylaminophenyl) diselenide (2) (20.35 g, 44.8 mmol) in 100.0 mL of 1.0 M HCl for 10 min. After another 10 min stirring, extract with dichloromethane (4 x 75.0 mL) and wash the organic phase twice with

brine. After being dried over anhydrous Na_2SO_4 , the solvent was distilled *in vacuo* to obtain a crude solid, which was recrystallized in isopropanol to afford an orange powder (16.35 g, 71%).

2.5. Synthesis of 1-naphthylamine derivatives (4a-d)

The synthetic method for compounds 4a-d have been described in the literature [33].

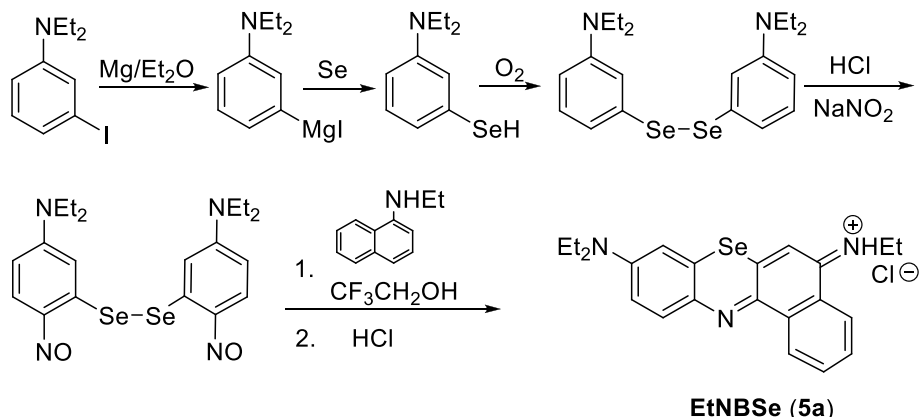
2.6. General procedure for the synthesis of benzo[a] phenoselenazinium dyes 5a-d

Benzo[a]phenoselenazinium dyes 5a-d were synthesized from bis-(3-diethylamino-6-nitrosophenyl) diselenide and the corresponding 1-naphthylamine derivatives (4a-d). Compound 3 (4.62 g, 9.0 mmol) was mixed with the corresponding 1-naphthylamine derivatives 4a-d (26.0 mmol) in 60.0 mL of trifluoroethanol, and the mixture was refluxed for 30 min. The solvent was then removed *in vacuo* to obtain a blue residue, which was subsequently washed with 60.0 mL of ethyl ether. The resultant residue was dissolved in 300.0 mL of a mixture containing 1.0 M aqueous sodium hydroxide solution and dichloromethane (1:1, v/v). The organic phase was washed twice with brine; after that, concentrated hydrochloric acid (0.1 mL) was added to the solution, which caused the solution color to change from magenta to dark blue. The solvent was removed *in vacuo* to obtain a blue residue, which was then purified by flash silica gel column using a solvent gradient of methanol/dichloromethane (0:100, 1:50, 1:30, 1:20, and 1:10, v/v) to yield the product.

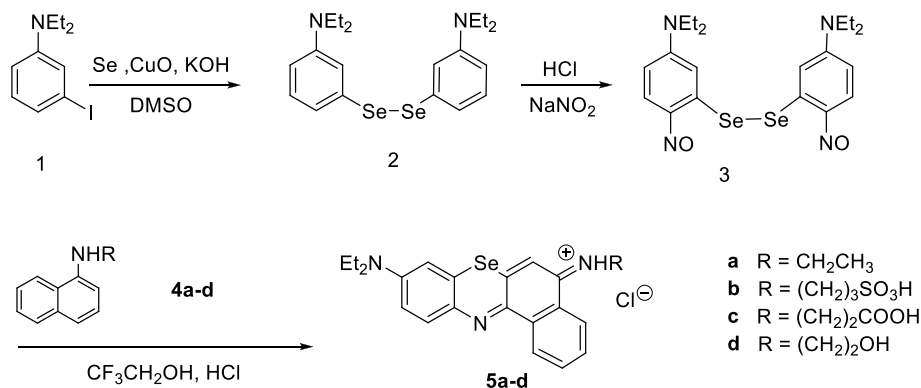
5a. Blue solid, yield: 41%. HRMS (ESI) m/z : calcd for $\text{C}_{22}\text{H}_{24}\text{N}_3\text{Se}$ $[\text{M}]^+$, 410.1130; found, 410.1123. ^1H NMR (400 MHz, $\text{DMSO}-d_6$) δ 10.48 (s, 1H), 8.73 (d, $J = 5.2$ Hz, 1H), 8.62 (s, 1H), 7.89–7.76 (m, 1H), 7.65 (d, $J = 4.5$ Hz, 2H), 7.19 (d, $J = 8.3$ Hz, 1H), 7.13 (s, 1H), 7.01 (s, 1H), 3.70 (s, 6H), 1.48 (d, $J = 5.8$ Hz, 2H), 1.42–1.30 (m, 6H). ^{13}C NMR (100 MHz, CDCl_3) δ 152.9, 150.3, 143.5, 138.7, 134.4, 133.7, 132.7, 131.96, 130.8, 129.4, 125.3, 124.4, 123.8, 115.8, 107.6, 105.9, 45.7, 39.3, 14.1, 12.7.

5b. Blue solid, yield: 40%. HRMS (ESI) m/z : calcd for $\text{C}_{23}\text{H}_{26}\text{N}_3\text{O}_3\text{SSe}$ $[\text{M}]^+$, 504.0855; found, 504.0354. ^1H NMR (400 MHz, $\text{DMSO}-d_6$) δ 10.20 (s, 1H), 8.99 (dd, $J = 8.2, 1.1$ Hz, 1H), 8.62 (d, $J = 8.1$ Hz, 1H), 8.02 (d, $J = 9.4$ Hz, 1H), 7.95 (s, 1H), 7.91 (t, $J = 7.6$ Hz, 1H), 7.85–7.79 (m, 1H), 7.73 (d, $J = 2.7$ Hz, 1H), 7.31 (dd, $J = 9.5, 2.7$ Hz, 1H), 3.73 (dd, $J = 14.3, 7.1$ Hz, 2H), 3.64 (q, $J = 6.9$ Hz, 4H), 1.37 (t, $J = 7.2$ Hz, 4H), 1.24 (t, $J = 7.0$ Hz, 6H). ^{13}C NMR (100 MHz, CDCl_3) δ 153.2, 150.9, 144.0, 139.3, 134.9, 133.9, 132.6, 131.2, 129.7, 125.8, 124.7, 123.3, 116.5, 108.0, 106.0, 46.0, 39.6, 29.9, 14.1, 12.9.

5c. Blue solid, yield: 38%. HRMS (ESI) m/z : calcd for $\text{C}_{23}\text{H}_{24}\text{N}_3\text{O}_2\text{Se}$ $[\text{M}]^+$, 454.1028; found, 454.1020. ^1H NMR (400 MHz, $\text{DMSO}-d_6$) δ 8.63 (d, $J = 7.7$ Hz, 1H), 8.34 (d, $J = 7.3$ Hz, 1H), 7.62 (dd, $J = 17.0, 7.3$ Hz,



Scheme 1. Schematic diagram showing the previous synthetic route of photosensitizer EtNBSe (5a).



Scheme 2. The improved synthetic route of the photosensitizers **5a-d** presented in this work.

4H), 7.11 (s, 1H), 6.85 (d, $J = 8.3$ Hz, 1H), 3.80 (t, $J = 6.6$ Hz, 2H), 3.53–3.44 (m, 4H), 2.70 (t, $J = 6.5$ Hz, 2H), 1.16 (t, $J = 6.9$ Hz, 6H). ¹³C NMR (100 MHz, DMSO-*d*₆) δ 175.0, 156.2, 151.0, 145.2, 139.1, 134.6, 132.2, 132.1, 129.7, 125.9, 124.2, 124.1, 117.0, 115.8, 111.1, 109.3, 107.9, 55.4, 45.6, 29.5, 22.6, 19.0, 13.2.

5d. Blue solid, yield: 45%. HRMS (ESI) m/z : calcd for C₂₂H₂₄N₃OSe [M]⁺, 426.1079; found, 426.1072. ¹H NMR (400 MHz, DMSO-*d*₆) δ 10.08 (s, 1H), 9.00 (d, $J = 8.0$ Hz, 1H), 8.60 (d, $J = 8.1$ Hz, 1H), 8.08–7.98 (m, 2H), 7.91 (t, $J = 7.6$ Hz, 1H), 7.83 (t, $J = 7.2$ Hz, 1H), 7.71 (s, 1H), 7.30 (d, $J = 9.3$ Hz, 1H), 5.14 (s, 1H), 3.79 (d, $J = 2.4$ Hz, 4H), 3.64 (q, $J = 6.9$ Hz, 4H), 1.24 (t, $J = 7.0$ Hz, 6H). ¹³C NMR (100 MHz, CDCl₃) δ 157.3, 154.6, 147.5, 142.9, 138.5, 137.7, 137.4, 136.4, 134.7, 133.1, 129.3, 128.2, 126.5, 120.3, 111.7, 110.2, 63.6, 50.5, 49.6, 16.3.

2.7. Measurement of singlet oxygen quantum yield (Φ_{Δ})

The ¹O₂ quantum yields (Φ_{Δ}) of the photosensitizers were determined with methylene blue (MB) as a reference ($\Phi_{\Delta} = 0.5$ in methanol) [34]. 1,3-Diphenylisobenzofuran (DPBF) in air-saturated dichloromethane with an optical density (OD) at 1.0 was used to scavenge ¹O₂. The concentration of the photosensitizer was adjusted to an OD between 0.2 and 0.3. The cuvette was irradiated for 10 s with monochromatic light at the maximum absorption wavelength of photosensitizers, and the absorbance was measured several times after each irradiation. The slope of the plot between the absorbance of DPBF at 411 nm versus time for each photosensitizer was calculated. Singlet oxygen quantum yield (Φ_{Δ}) was calculated according to a modified equation: $\Phi_{\Delta}^{\text{bod}} = \Phi_{\Delta}^{\text{ref}} * (k_{\text{bod}}/k_{\text{ref}}) * (F_{\text{ref}}/F_{\text{bod}})$, where bod and ref refer to the photosensitizers and MB, respectively, k is the slope of the plot between the absorbance of DPBF (411 nm) versus irradiation time, and F is the absorption correction factor (which was calculated by $F = 1 - 10^{-\text{O.D.}}$, where O.D. is the optical density of the solution at the irradiation wavelength).

2.8. In vitro toxicity assay

MTT assay was used to assess the toxicity to cancer cells of the photosensitizers [32]. HepG2 cells (100.0 μL ; density = 5000 cells/mL) in the logarithmic phase were added to 96-well plates and incubated at 37 °C in 5% CO₂ for 24 h. After that, 100.0 μL of each of the photosensitizers **5a-d** in DMSO solution was added to each well, and cells were further incubated for 1 h. After being illuminated with 660 nm LED light (20 mW/cm²), cells were incubated for 24 h at 37 °C in 5% CO₂ atmosphere. Subsequently, the medium in each well was replaced with 100.0 μL of fresh medium, and 20.0 μL of MTT solution was added thereafter. After the culture plates were then incubated at 37 °C in 5% CO₂ for 4 h, the culture medium was discarded, and 100.0 μL of DMSO was added. The absorbance at 570 nm of the samples was measured using a microplate reader. Cells incubated with photosensitizers without light irradiation were used as a control.

3. Results and discussion

3.1. Chemistry of the synthesis

In this study, bis-(3-diethylamino-6-nitrosophenyl) diselenide was synthesized in one step using CuO nanopowder as a catalyst. This new synthetic method had several advantages as follows: (i) the special care needed for the Grignard reaction was avoided; (ii) the toxic selenium vapor was not generated because air bubbles were omitted; and (iii) the reaction procedure was simple (as it could be accomplished in only one step), and the product yield was improved from 56% to 74.5% without the need of column chromatography. Thus, this new synthetic method was able to readily prepare four pure benzo[*a*]phenoselenazinium dyes **5a-d** with high yields.

3.2. Optical properties of photosensitizers

We determined the optical spectra of the four photosensitizers **5a-d** in methanol and H₂O. All the dyes contain a delocalized positive charge and are soluble in methanol and H₂O. The four dyes exhibited an intensive absorption band within the optical window ($\lambda_{\text{max}} \approx 660$ nm; Fig. 1). In H₂O, the dyes exhibited an absorption band at about 627 nm, which might be caused by H-aggregation of the photosensitizers [25]. As expected, the dyes also exhibited weak fluorescence due to the effect of the heavy metal Se [35,36] (Fig. 1).

3.3. Singlet oxygen quantum yield

The singlet oxygen quantum yields of the photosensitizers **5a-d** in methanol were measured using the ¹O₂ trapping reagent 1,3-diphenylisobenzofuran (DPBF). As shown in Fig. 2 and S2, illuminating the solutions of the photosensitizers **5a-d** in DPBF with 660 nm LED light caused their absorption intensity at 411 nm to decrease due to the irreversible 1,4-cycloaddition reaction between DPBF and ¹O₂. Moreover, with increasing illumination time, the decrease was intensified. The singlet oxygen yields of the photosensitizers **5a-d** were determined to be over 0.8 (Table 1).

3.4. In vitro photodynamic therapy and imaging

HepG2 cells were cultured with photosensitizers **5a-d** for 30 min; after that, they were irradiated under a 660 nm light (20 mW/cm²) for 0, 1, 5, and 10 min, respectively; non-irradiated samples were also prepared for comparison. As shown in Fig. 3, the non-irradiated photosensitizers **5a-d** were non-toxic, suggesting they have good biocompatibility *in vitro*. In contrast, as expected, the light-irradiated photosensitizers **5a-d** were highly cytotoxic, and the cytotoxicity increased with increasing the dose of photosensitizer as well as with the irradiation time. Interestingly, photosensitizers **5a**, **5b** and **5d** at a low

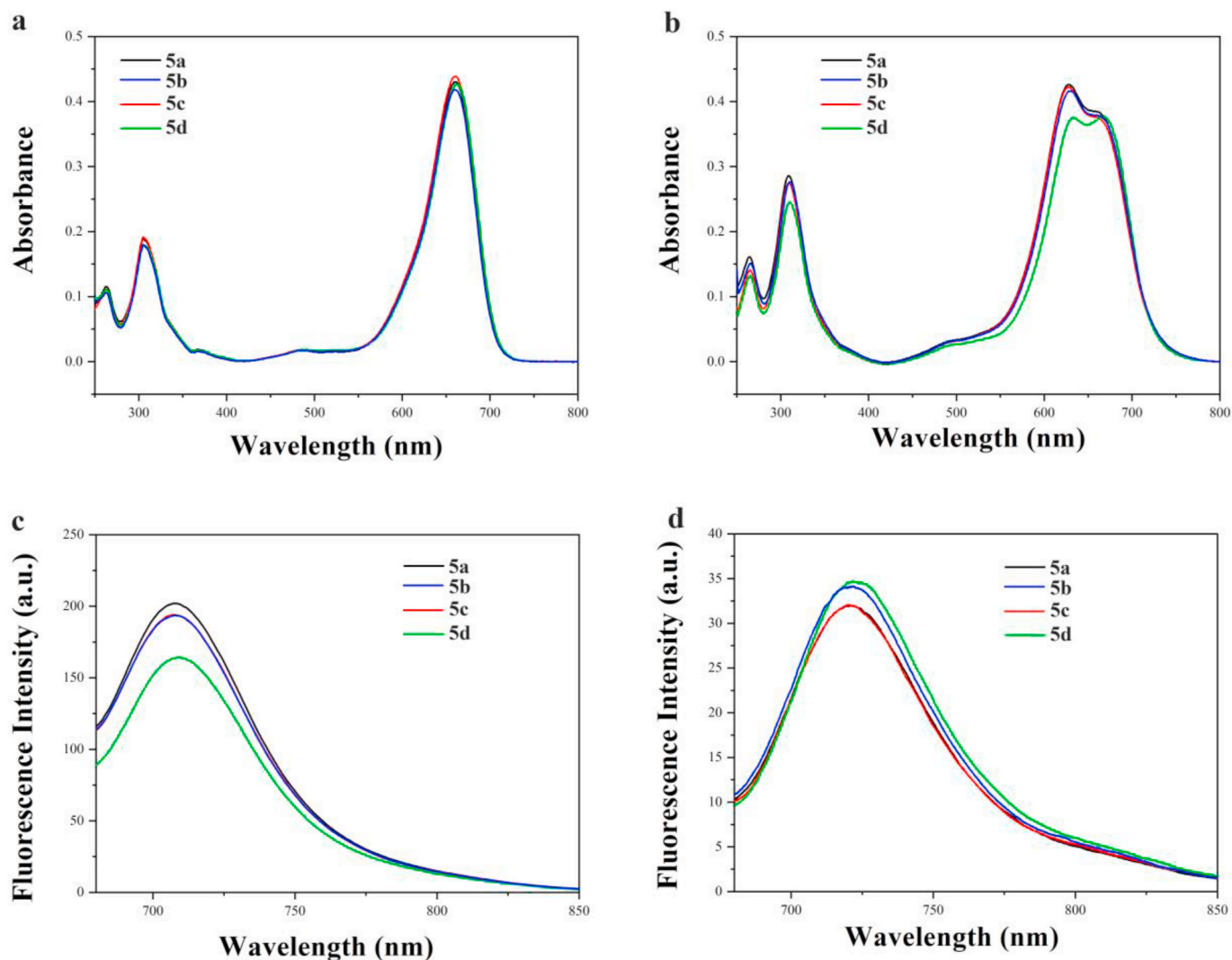


Fig. 1. Absorption (top row) and fluorescence (bottom row) spectra of photosensitizers **5a-d** in methanol (a, c) and in H₂O (b, d).

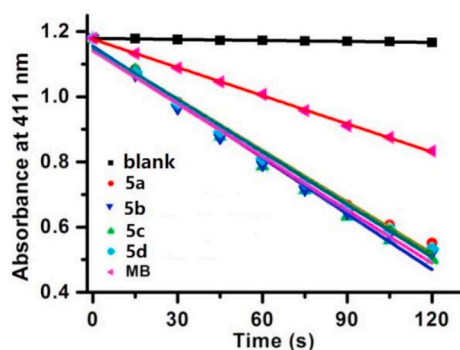


Fig. 2. The decay curves of the absorbance at 411 nm of DPBF in methanol as a function of irradiation time without and with photosensitizers **5a-d** and methylene blue (MB). Light source 660 nm LED (20 mW/cm²).

concentration of 0.04 μ M displayed high cytotoxicity when the irradiation time was 10 min; however, this is not the case for photosensitizer **5c**. As shown in Fig. S4, these four dyes all exhibited bright red fluorescence in HepG2 cells. These results indicate that photosensitizers **5a-d** had good photodynamic therapeutic effect and could also be applied for cell imaging.

Table 1
Photophysical properties of photosensitizers **5a-d** in methanol.

Compounds	$\lambda_{\text{abs}}/\text{nm}$	$\lambda_{\text{em}}/\text{nm}$	$\Phi_{\Delta} (^1\text{O}_2)$
5a	660	707	0.80
5b	660	707	0.83
5c	660	708	0.86
5d	660	708	0.86

4. Conclusion

In conclusion, CuO nanopowder was used as the catalyst to optimize the synthesis of the key intermediate of benzo[*a*]phenoselenazinium PDT agents, bis-(3-diethylaminophenyl) diselenide. This new synthetic method required a mild reaction condition, but resulted in the product with high purity without the need of purification by column chromatography; it also had a simple and straightforward operation procedure. This work presents the synthesis method for benzo[*a*]phenoselenazinium PDT agents that can be potentially up-scaled. With this method, the clinical studies and practical applications of the agents can potentially be boosted.

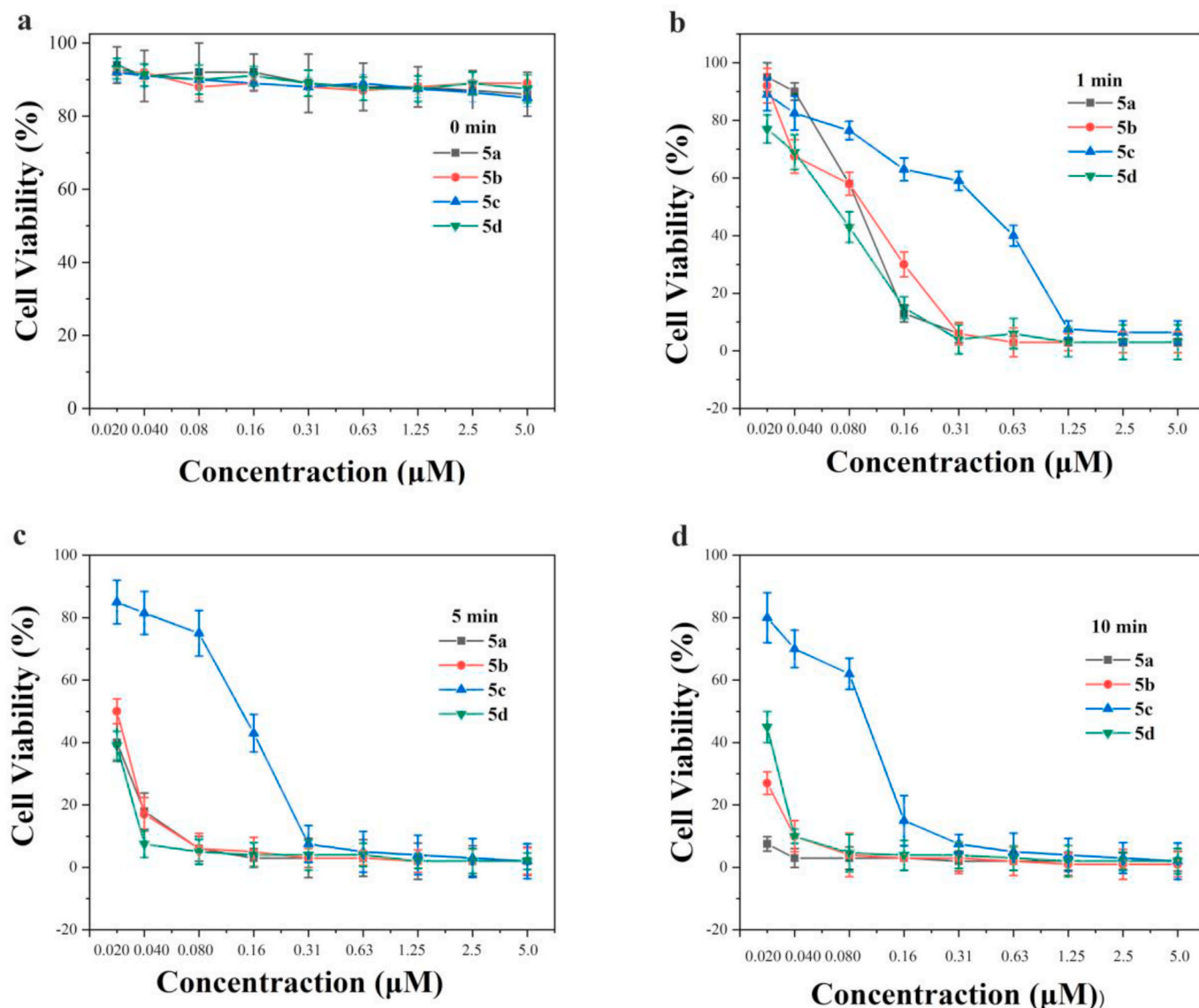


Fig. 3. Cytotoxicity against HepG2 cells of photosensitizers 5a-d at various concentrations under a 660 nm light (20 mW/cm^2) irradiation for (a) 0 min, (b) 1 min, (c) 5 min, and (d) 10 min.

Credit author statement

Xiuxiu Yue prepared the photosensitizers 5a-d, performed the measurements, analyzed the data, and wrote the paper. Jing Xu prepared the performed the experiments. Xiangzhi Song processed the data and writing-review & editing supervision with Xiaozhong Liu and James W. Foley. All authors have given approval to the final version of the paper.

Funding sources

This work was supported by the Natural Science Foundation of Hunan Province, China (No. 2019JJ40360), National Natural Science Foundation of China (No. 21907110) and Basic Research Foundation of Shenzhen Science and Technology Innovation (No. JCYJ20190806144605441).

Declaration of competing interest

The authors declare that they have no known competing financial interests or personal relationships that could have appeared to influence the work reported in this paper.

Appendix A. Supplementary data

Supplementary data to this article can be found online at <https://doi.org/10.1016/j.dyepig.2021.109154>.

References

- [1] Zhang Y, Shen W, Zhang P, Chen L, Xiao C. GSH-triggered release of sulfur dioxide gas to regulate redox balance for enhanced photodynamic therapy. *Chem Commun* 2020;56:5645–8.
- [2] Ferraz RC, Fontana CR, Ribeiro AP, Trindade FZ, Bartoloni FH, Baader JW, Lins EC, Bagnato VS, Kurachi C. Chemiluminescence as a PDT light source for microbial control. *J Photochem Photobiol, B* 2011;103:87–92.
- [3] Hu W, He T, Zhao H, Tao H, Chen R, Jin L, Li J, Fan Q, Huang W, Baev A, Prasad PN. Stimuli-responsive reversible switching of intersystem crossing in pure organic material for smart photodynamic therapy. *Angew Chem Int Ed* 2019;58:11105–11.
- [4] Demir Duman F, Sebek M, Thanh NTK, Loizidou M, Shakib K, MacRobert AJ. Enhanced photodynamic therapy and fluorescence imaging using gold nanorods for porphyrin delivery in a novel in vitro squamous cell carcinoma 3D model. *J Mater Chem B* 2020;8:5131–42.
- [5] Rizvi I, Anbil S, Alagic N, Celli J, Zheng LZ, Palanisami A, Glidden MD, Pogue BW, Hasan T. PDT dose parameters impact tumoricidal durability and cell death pathways in a 3D ovarian cancer model. *Photochem Photobiol* 2013;89:942–52.

- [6] Famularo G, De Simone C. HIV infection of CD8 lymphocytes: a critical step for the disease? *Nat Rev Canc* 1998;13:65–6.
- [7] Bachor R, Shea CR, Gillies R, Hasan T. Photosensitized destruction of human bladder carcinoma cells treated with chlorin e6-conjugated microspheres. *Proc Natl Acad Sci USA* 1991;88:1580.
- [8] Celli JP, Spring BQ, Rizvi I, Evans CL, Samkoe KS, Verma S, Pogue BW, Hasan T. Imaging and photodynamic therapy: mechanisms, monitoring, and optimization. *Chem Rev* 2010;110:2795–838.
- [9] Lovell JF, Liu TWB, Chen J, Zheng G. Activatable photosensitizers for imaging and therapy. *Chem Rev* 2010;110:2839–57.
- [10] Li M, Xia J, Tian R, Wang J, Fan J, Du J, Long S, Song X, Foley JW, Peng X. Near-infrared light-initiated molecular superoxide radical generator: rejuvenating photodynamic therapy against hypoxic tumors. *J Am Chem Soc* 2018;140:14851–9.
- [11] Li M, Xiong T, Du J, Tian R, Xiao M, Guo L, Long S, Fan J, Sun W, Shao K, Song X, Foley JW, Peng X. Superoxide radical photogenerator with amplification effect: surmounting the achilles' heels of photodynamic oncology. *J Am Chem Soc* 2019;141:2695–702.
- [12] Jiang Y, Li J, Zeng Z, Xie C, Lyu Y, Pu K. Organic photodynamic nanoinhibitor for synergistic cancer therapy. *Angew Chem Int Ed* 2019;58:8161–5.
- [13] Chen H, Li S, Wu M, Kenry, Huang Z, Lee CS, Liu B. Membrane-anchoring photosensitizer with aggregation-induced emission characteristics for combating multidrug-resistant bacteria. *Angew Chem Int Ed* 2020;59:632–6.
- [14] Cui D, Huang J, Zhen X, Li J, Jiang Y, Pu K. A semiconducting polymer nano-prodrug for hypoxia-activated photodynamic cancer therapy. *Angew Chem Int Ed* 2019;58:5920–4.
- [15] Viola G, Dall'Acqua F. Photosensitization of biomolecules by phenothiazine derivatives. *Curr Drug Targets* 2006;7:1135–54.
- [16] Azizi B, Budimir A, Bago I, Mehmeti B, Jakovljević S, Kelmendi J, Stanko AP, Gabrić D. Antimicrobial efficacy of photodynamic therapy and light-activated disinfection on contaminated zirconia implants: an in vitro study. *Photodiagnosis Photodyn Ther* 2018;21:328–33.
- [17] Castano AP, Mroz P, Hamblin MR. Photodynamic therapy and anti-tumour immunity. *Nat Rev Canc* 2006;6:535–45.
- [18] Shen Y, Shuhendler AJ, Ye D, Xu JJ, Chen HY. Two-photon excitation nanoparticles for photodynamic therapy. *Chem Soc Rev* 2016;45:6725–41.
- [19] Castano AP, Mroz P, Hamblin MR. Photodynamic therapy and anti-tumour immunity. *Nat Rev Canc* 2006;6:535–45.
- [20] Castano AP, Demidova TN, Hamblin MR. Mechanisms in photodynamic therapy: part two-cellular signaling, cell metabolism and modes of cell death. *Photodiagnosis Photodyn Ther* 2005;2:1–23.
- [21] Zheng X, Sallum UW, Verma S, Athar H, Evans CL, Hasan T. Exploiting a bacterial drug-resistance mechanism: a light-activated construct for the destruction of MRSA. *Angew Chem Int Ed* 2009;48:2148–51.
- [22] O'Riordan K, Akilov OE, Chang SK, Foley JW, Hasan T. Real-time fluorescence monitoring of phenothiazinium photosensitizers and their anti-mycobacterial photodynamic activity against *Mycobacterium bovis* BCG in in vitro and in vivo models of localized infection. *Photochem Photobiol Sci* 2007;6:1117–23.
- [23] Wagner SJ, Skripchenko A, Robinette D, Foley JW, Cincotta L. Factors affecting virus photoinactivation by a series of phenothiazine dyes. *Photochem Photobiol* 1998;67:343–9.
- [24] Akilov OE, Kosaka S, O'Riordan K, Song X, Sherwood M, Flotte TJ, Foley JW, Hasan T. The role of photosensitizer molecular charge and structure on the efficacy of photodynamic therapy against *Leishmania* parasites. *Chem Biol* 2006;13:839–47.
- [25] Foley JW, Song X, Demidova TN, Jilal F, Hamblin MR. Synthesis and properties of benzo[a]phenoxazinium chalcogen analogues as novel broad-spectrum antimicrobial photosensitizers. *J Med Chem* 2006;49:5291–9.
- [26] Vecchio D, Bhayana B, Huang L, Carrasco E, Evans CL, Hamblin MR. Structure-function relationships of Nile blue (EtNBS) derivatives as antimicrobial photosensitizers. *Eur J Med Chem* 2014;75:479–91.
- [27] Liu A, Zhang W, Chen Y, Zhou D, Wang Z, Kang J, Wei L. EtNBSe-PDT inhibited proliferation and induced autophagy of HNE-1 cells via downregulating the Wnt/ β -catenin signaling pathway. *Photodiagnosis Photodyn Ther* 2019;26:65–72.
- [28] Chen J, Huang J-H, Wang Z, Song X, Chen Z, Zeng Q, Zhou X, Zuo Z, Zhao S, Chen X, Kang J. Endoplasmic reticulum stress-mediated autophagy contributes to 5-ethylamino-9-diethylaminobenzo[a]phenoselenazinium-mediated photodynamic therapy via the PERK-eIF2 α pathway. *OncoTargets Ther* 2018;11:4315–25.
- [29] Kelland LR, Abel G, McKeage MJ, Jones M, Goddard PM, Valenti M, Murrer BA, Harrap KR. Preclinical antitumor evaluation of bis-acetato-ammine-dichloro-cyclohexylamine platinum(IV): an orally active platinum drug. *Canc Res* 1993;53:2581–6.
- [30] Akilov OE, Kosaka S, O'Riordan K, Hasan T. Photodynamic therapy for cutaneous leishmaniasis: the effectiveness of topical phenothiaziniums in parasite eradication and Th1 immune response stimulation. *Photochem Photobiol Sci* 2007;6:1067–75.
- [31] Cincotta L, Szeto D, Lampros E, Hasan T, Cincotta AH. Benzophenothiazine and benzoporphyrin derivative combination phototherapy effectively eradicates large murine sarcomas. *Photochem Photobiol* 1996;63:229–37.
- [32] Cincotta L, Foley JW, Cincotta AH. Novel red absorbing benzo[a]phenoxazinium and benzo[a]phenothiazinium photosensitizers: in vitro evaluation. *Photochem Photobiol* 1987;46:751–8.
- [33] Frade VHJ, Barros SA, Moura JCVP, Coutinho PJG, Gonçalves MST. Synthesis of short and long-wavelength functionalised probes: amino acids' labelling and photophysical studies. *Tetrahedron* 2007;63:12405–18.
- [34] Detty MR, Merkel PB. Chalcogenopyrylium dyes as potential photochemotherapeutic agents. Solution studies of heavy atom effects on triplet yields, quantum efficiencies of singlet oxygen generation, rates of reaction with singlet oxygen, and emission quantum yields. *J Am Chem Soc* 1990;112:3845–55.
- [35] Ohulchanskyy TY, Donnelly DJ, Detty MR, Prasad PN. Heteroatom substitution induced changes in excited-state photophysics and singlet oxygen generation in chalcogenoxanthylum dyes: effect of sulfur and selenium substitutions. *J Phys Chem B* 2004;108:8668–72.
- [36] Piao W, Hanaoka K, Fujisawa T, Takeuchi S, Komatsu T, Ueno T, Terai T, Tahara T, Nagano T, Urano Y. Development of an azo-based photosensitizer activated under mild hypoxia for photodynamic therapy. *J Am Chem Soc* 2017;139:13713–9.